

Short communication

Effect of Al-substitution on the stability of LiMn_2O_4 spinel, synthesized by citric acid sol–gel method

B.J. Hwang^{*}, R. Santhanam, D.G. Liu, Y.W. Tsai

Microelectrochemistry Laboratory, Department of Chemical Engineering, National Taiwan University of Science and Technology, 43 Keelung Road, Section 4, 106 Taipei, Taiwan, ROC

Received 21 February 2001; accepted 21 March 2001

Abstract

Spinel LiMn_2O_4 and $\text{LiAl}_x\text{Mn}_{2-x}\text{O}_4$ ($x = 0.05, 0.15$) are synthesized by a sol–gel method using citric acid as a chelating agent. The effect of calcination temperature on the purity of the Al-substituted spinel is examined by X-ray diffraction measurements which suggests that pure material is obtained by calcination at 800°C . Cyclic voltammetry is employed to characterize the reactions of lithium insertion into and extraction from the spinel materials. Surface morphology changes are observed by scanning electron microscopy (SEM) and transmission electron microscopy (TEM). The results indicate that Al-substitution enhances sintering of the spinel LiMn_2O_4 . Charge–discharge cycling studies show that Al-substitution improves substantially the capacity retention of the spinel LiMn_2O_4 . © 2001 Elsevier Science B.V. All rights reserved.

Keywords: Spinel LiMn_2O_4 ; Al-substitution; Capacity retention; Lithium batteries

1. Introduction

Spinel LiMn_2O_4 , because of its easy preparation, and its economical and environmental advantages, is considered to be a promising material for the positive electrode (cathode) of secondary lithium batteries [1–5]. It is seen as possible alternative to LiCoO_2 which is presently the favoured material. The capacity of spinel LiMn_2O_4 , however, fades rapidly on charge–discharge cycling. It has been suggested that the capacity fading in the 3 V region is due to Jahn–Teller distortion [2] and in the 4 V region due to dissolution of spinel into the electrolyte and decomposition of the electrolyte [6–8]. It is also proposed that the inferior cycleability of LiMn_2O_4 is due to cation mixing between Li and Mn ions in the spinel lattice [9,10], breakdown of the spinel lattice [11,12], and oxygen loss from the spinel lattice [13–15]. Extensive studies have been directed towards various strategies to improve the cycleability of LiMn_2O_4 . Among these, one effective approach is to substitute a small amount of dopant ions in place of Mn ions [16–19]. It is believed that the dopant ions are occupied in the 16d sites of the Mn ions in the spinel lattice and stabilize the structure.

The sol–gel method for preparing LiMn_2O_4 has several advantages, such as a low calcination temperature, a short processing time, and submicron-sized particles with a narrow particle-size distribution. In the present work, the sol–gel method has been used to synthesize spinel LiMn_2O_4 and Al-doped spinel LiMn_2O_4 . The synthesis of nanoparticles of the spinel LiMn_2O_4 by the citric acid sol–gel method and the effect of various synthetic parameters on the purity of the spinel LiMn_2O_4 have been reported in our previous studies [20,21]. The aim of the present work is to study the effect of Al-doping on the surface morphology and the electrochemical stability of the spinel.

2. Experimental

LiMn_2O_4 and $\text{LiAl}_x\text{Mn}_{2-x}\text{O}_4$ were synthesized by the sol–gel method using citric acid as a chelating agent. Stoichiometric amounts of lithium, manganese and aluminium acetate salts were first dissolved in deionized water. To this solution, a saturated aqueous solution of citric acid was then added with stirring. In all the experiments, the molar ratio of chelating agent to the total metal ions was unity. The pH of the mixed solution was maintained between 6.4 and 6.8 by the addition of ammonium hydroxide solution. The mixtures were stirred with gentle

^{*} Corresponding author. Tel.: +886-2-273-766-24;
fax: +886-2-273-766-44.
E-mail address: bjh@ch.ntust.edu.tw (B.J. Hwang).

heating for 4 h to remove excess ammonia and water. The resulting precipitate of metal citrate was dried in an air oven for 10 h at 100°C. After drying, the precursors were decomposed at 300°C for 6 h in air to eliminate organic contents. The decomposed powders were slightly ground and then calcined at various temperatures. During heating and cooling, the variation the temperature was fixed as 1°C/min.

Composite cathodes of LiMn_2O_4 and $\text{LiAl}_x\text{Mn}_{2-x}\text{O}_4$ were prepared from their respective slurries which contained 80 wt.% sample, 10wt.% PVDF (Aldrich) and 10 wt.% carbon black (Acros) dissolved in *N*-methyl-2-pyrrolidinone (NMP, Aldrich). The slurry was then cast on to an aluminium foil (Aldrich, 99.9%, 0.05 mm thick) by means of a coater, dried at 120°C under vacuum for 4 h and then roll-pressed. The procedure resulted in the formation of a composite cathode film.

LiMn_2O_4 and $\text{LiAl}_x\text{Mn}_{2-x}\text{O}_4$ samples were characterized by powder X-ray diffractometry (XRD) using a Rigaki instrument with Cu K α radiation. The chemical composition of the samples was analyzed by means of inductively coupled plasma–atomic emission spectroscopy (ICP–AES) measurements. The compositions of the Al-substituted spinel samples were determined to be $\text{Li}_{0.98}\text{Al}_{0.05}\text{Mn}_{1.95}\text{O}_4$ and $\text{Li}_{0.946}\text{Al}_{0.147}\text{Mn}_{1.85}\text{O}_4$. The morphology and particle size of the sample were investigated both by scanning electron microscopy (SEM, Hitachi S-2400) and transmission electron microscopy (TEM, JEOL JSM 1200 Ex-II). Cyclic voltammograms of the samples were obtained in a three-electrode cell at a scan rate of 0.02 V s⁻¹ using a potentiostat (Autolab, eco chemie).

Reference and counter electrodes were fabricated from lithium metal. Cycling tests were carried out on a coin-type cell of Li/1 M LiPF_6 in ethylene carbonate and diethyl carbonate (EC-DEC 1:1 v/v)/ LiMn_2O_4 or $\text{LiAl}_x\text{Mn}_{2-x}\text{O}_4$. The cell was assembled in an argon-filled glove box (Mbraun) in which both the moisture and the oxygen levels were less than 1 ppm. The cells thus fabricated were cycled galvanostatically in the voltage range 3.3–4.3 V, at 0.1 C rate. The charge and discharge capacities were measured at room temperature with an Arbin battery tester system (ABTS).

3. Results and discussion

The XRD patterns for $\text{LiAl}_{0.15}\text{Mn}_{1.85}\text{O}_4$ at various calcination temperatures are shown in Fig. 1 (note, a similar pattern was given by $\text{LiAl}_{0.05}\text{Mn}_{1.95}\text{O}_4$). As the heat-treatment temperature increases, the XRD peaks are enhanced. An impurity peak, indicated by asterisk (*), is observed at temperature between 500 and 700°C (since the relative intensity of the impurity is very low, impurity peaks are not observed at 300 and 400°C). At 800°C, however, the Al-substituted spinel is found to be pure and more crystalline, as demonstrated by the sharper intensities of all the

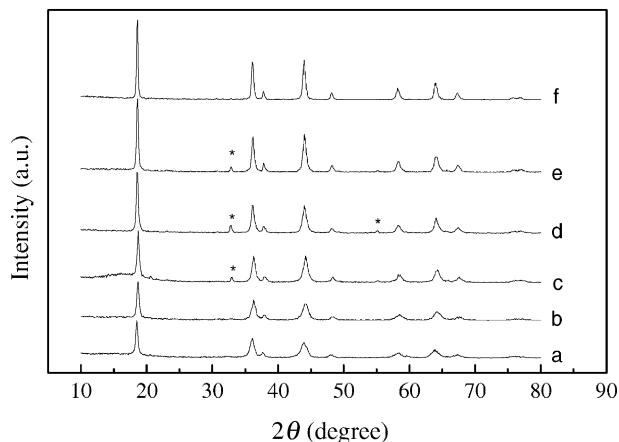


Fig. 1. XRD patterns of $\text{LiAl}_{0.15}\text{Mn}_{1.85}\text{O}_4$ samples synthesized at various temperatures: (a) 300°C; (b) 400°C; (c) 500°C; (d) 600°C; (e) 700°C; (f) 800°C. Asterisk (*) indicates Mn_2O_3 impurity.

peaks. Hence, Al-substituted spinels calcined at 800°C were used in subsequent studies. In order to determine the relationship between calcination time and particle growth, the particle size of Al-substituted spinels calcined at various

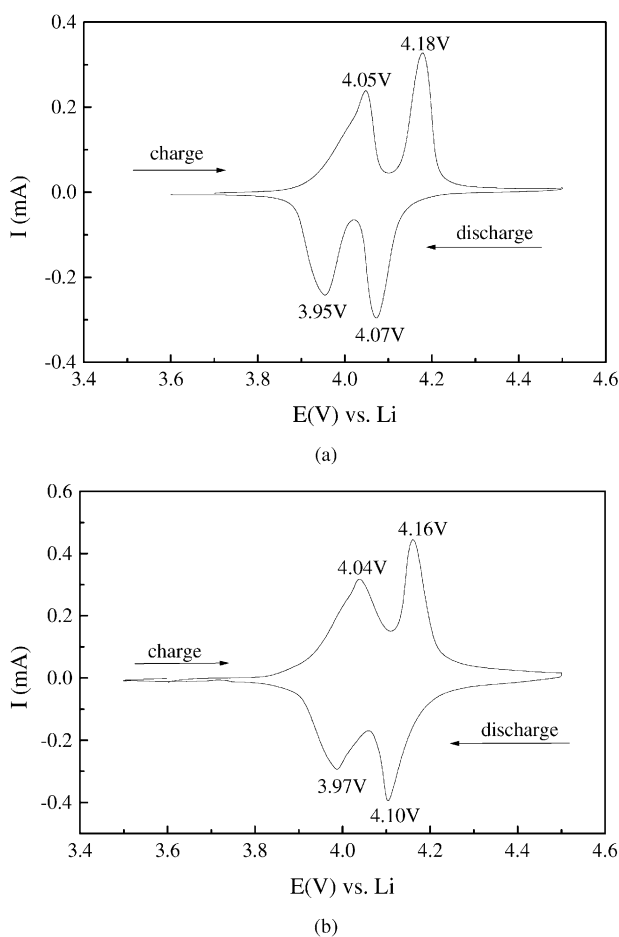


Fig. 2. Cyclic voltammograms of (a) LiMn_2O_4 and (b) $\text{LiAl}_{0.15}\text{Mn}_{1.85}\text{O}_4$ prepared at 800°C for 10 h. Electrolyte solution: 1 M LiPF_6 in 1:1 mixture of EC and DEC; scan rate: 0.02 mV s⁻¹.

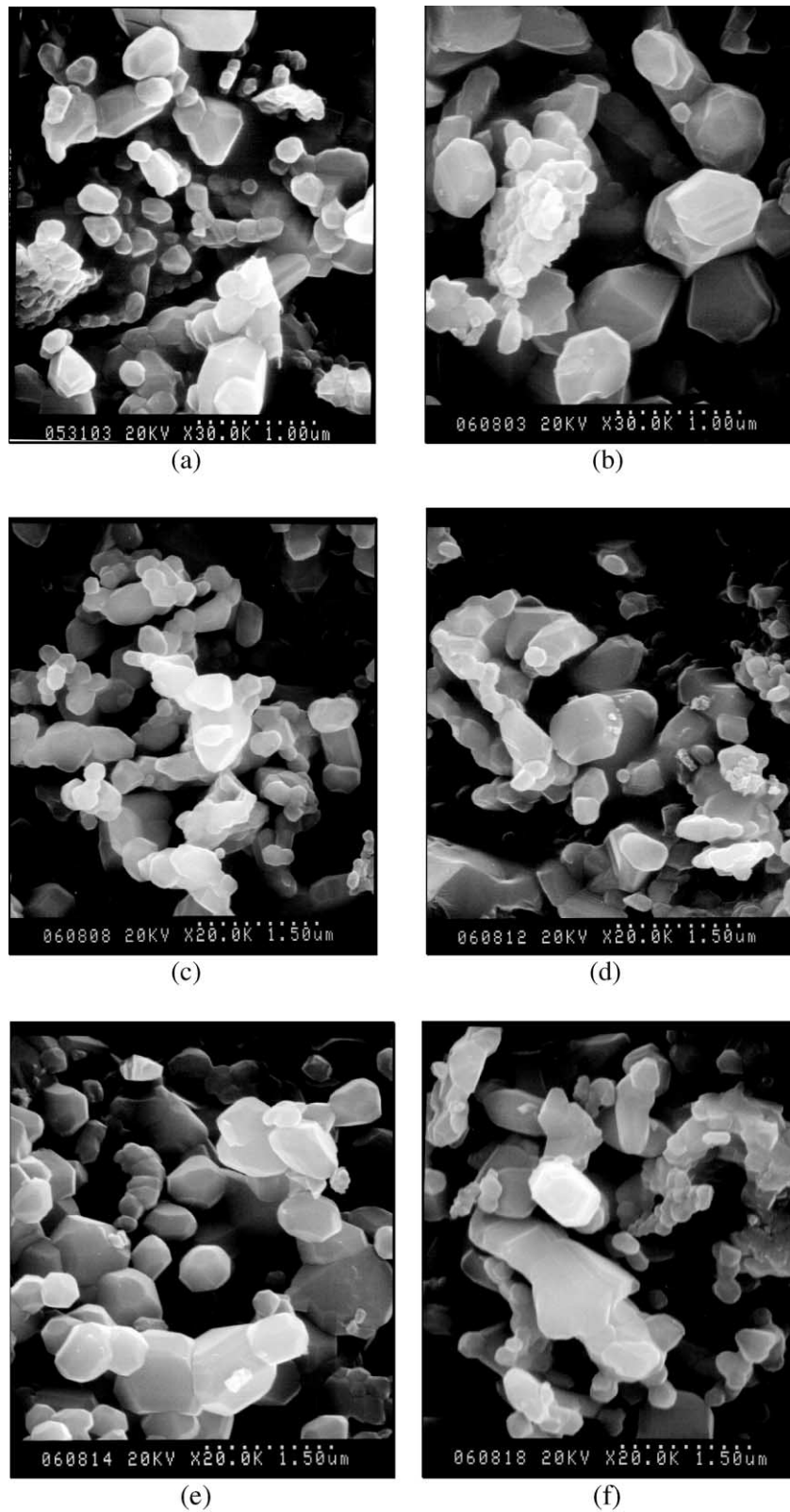


Fig. 3. Scanning electron micrographs of $\text{LiAl}_x\text{Mn}_{2-x}\text{O}_4$ synthesized at 800°C in air. Calcination time: (a), (b) 10 h; (c), (d) 15 h; (e), (f) 20 h. Al-substitution ratio for (a), (c), (e) and (b), (d), (f) is 0.05 and 0.15, respectively.

temperatures was determined from XRD patterns using Scherrer's formula

$$t = 0.9\lambda / B \cos \theta \quad (1)$$

where λ , B , and θ are the wavelength of X-ray used, the full wave at half-intensity maximum and the Bragg angle of the given diffraction peak, respectively. The particle size is found to increase with the calcination time. For example, the particle size of the sample $\text{LiAl}_{0.05}\text{Mn}_{1.95}\text{O}_4$ prepared at

800°C for 10, 15 and 20 h is calculated as 44, 47, 49 nm, respectively.

Cyclic voltammetric measurements were made for the spinel LiMn_2O_4 and Al-substituted spinel, $\text{LiAl}_{0.15}\text{Mn}_{1.85}\text{O}_4$ over the potential range 3.6–4.5 V at a scan rate of 0.02 mV s^{-1} . The first charge and the subsequent discharge curves for these two spinels are shown in Fig. 2(a) and (b), respectively. While the shape of the cyclic voltammetric peaks broadens and the peak currents increase to some

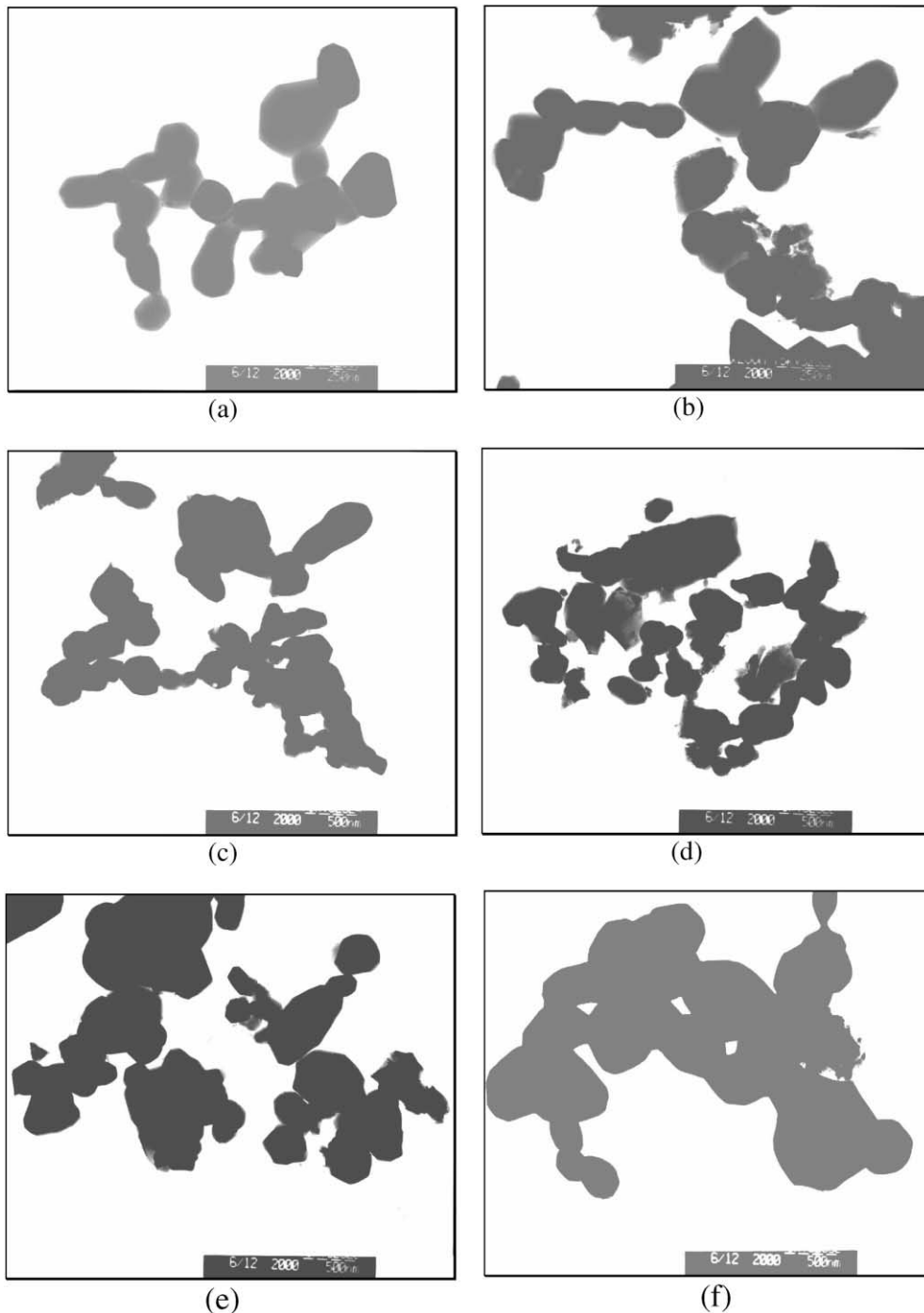


Fig. 4. Transmission electron micrographs for same samples as those used to produce Fig. 3.

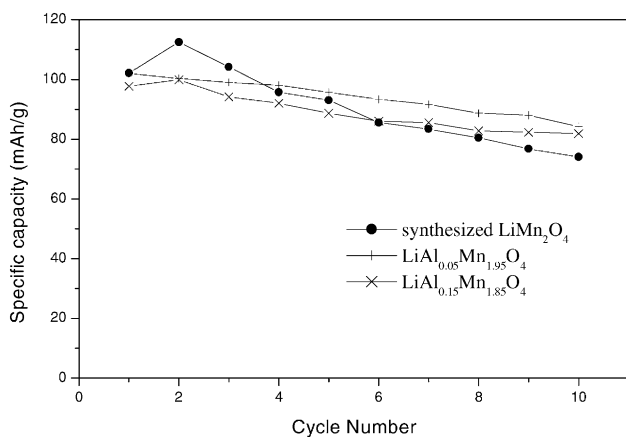


Fig. 5. Discharge capacity vs. cycle number for the spinel and Al-substituted spinel LiMn_2O_4 synthesized at 800°C for 10 h.

extent, the essential voltmmetric features are the same for the two spinels. For unsubstituted spinel, the oxidation peaks are located at about 4.05 and 4.18 V, and the reduction peaks at 3.95 and 4.07 V, respectively. For the Al-substituted spinel, the peaks are located in similar potential regions with a difference of only a few millivolts. The symmetry of the anodic and cathodic peaks reflect the reversibility of the oxidation and reduction reactions that correspond to lithium extraction and insertion.

The effects of aluminium substitution ratio and calcination time on the morphology of the Al-substituted spinel LiMn_2O_4 were examined by scanning electron microscopy (SEM) and transmission electron microscopy (TEM). The SEM and TEM micrographs were recorded for the Al-doped samples with two different substitution ratios (0.05 and 0.15) and calcined at 800°C for various times (10, 15, and 20 h). SEM micrographs (Fig. 3(a)–(f)) show that the particle size is somewhat larger for the spinel with a 0.15 ratio of aluminium substitution than that with a 0.05 ratio at all the calcination times studied. In all the micrographs, the particles of the Al-doped spinel show good crystallinity and uniformity. TEM micrographs (Fig. 4(a)–(f)) also show larger particle size when the aluminium doping ratio is higher at all calcination times. As the calcination time is increased, particle agglomeration is also found to increase due to a higher degree of crystallization. From these SEM and TEM results, it is concluded that Al-substitution enhances the sintering of LiMn_2O_4 . The variations of discharge capacity with cycle number for spinel LiMn_2O_4 , and Al-substituted spinel $\text{LiAl}_{0.05}\text{Mn}_{1.95}\text{O}_4$ and $\text{LiAl}_{0.15}\text{Mn}_{1.85}\text{O}_4$ are shown in Fig. 5. The capacity retention of the Al-substituted spinels is enhanced in comparison with that of LiMn_2O_4 . The observed behavior may be due to two reasons. First, there may be a considerable decrease in the effect of Jahn–Teller distortion when substituting a small amount of Al for Mn in the spinel. This means that the concentration of Mn^{3+} which induces Jahn–Teller distortion in the spinel is decreased. Second, there may be a reduction in spinel dissolution. It has already been established that the solvent oxidation potential

plays an important role in spinel dissolution [7,8] Substitution of small amount of Al for Mn may shift the solvent oxidation to a higher anodic potential. As a consequence the acids generated as a result of solvent oxidation would be decreased and hence the dissolution of the spinel would be decreased. Therefore, the structural stability of $\text{LiAl}_x\text{Mn}_{2-x}\text{O}_4$ due to Al substitution contributes to the reversibility of the charge–discharge cycles. The discharge capacity of $\text{LiAl}_{0.15}\text{Mn}_{0.85}\text{O}_4$ for the first and third cycles is somewhat less than that of $\text{LiAl}_{0.05}\text{Mn}_{1.95}\text{O}_4$ for the corresponding cycles. Although an increase in the ratio of aluminium increases the manganese oxidation state of the spinel $\text{LiAl}_{0.15}\text{Mn}_{0.85}\text{O}_4$, there is a greater decrease in the amount of Mn compared with the spinel $\text{LiAl}_{0.05}\text{Mn}_{1.95}\text{O}_4$. Hence, the capacity of the spinel $\text{LiAl}_{0.15}\text{Mn}_{0.85}\text{O}_4$ is somewhat smaller.

4. Conclusions

In this work, spinel LiMn_2O_4 and Al-substituted spinel $\text{LiAl}_x\text{Mn}_{2-x}\text{O}_4$ have been prepared by a citric acid sol–gel method and their surface and electrochemical properties have been examined. Cyclic voltammetric experiments reveal that the redox peaks are broadened and peaks currents increased after substitution of Mn by Al in the spinel LiMn_2O_4 structure. From SEM and TEM measurements it is found that the particle size increases with increase in substitution ratio of Al. This observation suggests that Al substitution enhances the sintering of LiMn_2O_4 . Charge and discharge cycling experiments show that the capacity retention of Al-substituted spinel is substantially better than that of LiMn_2O_4 .

Acknowledgements

Financial support from National Science Council (NSC-89-2214-E-011-044-) is gratefully acknowledged.

References

- [1] S. Magahed, B. Scrosati, J. Power Sources 51 (1994) 79.
- [2] T. Ohzuku, M. Kitagawa, T. Hirai, J. Electrochem. Soc. 137 (1990) 769.
- [3] Y. Xia, M. Yoshio, J. Power Sources 56 (1995) 61.
- [4] C. Sigala, D. Guyomard, A. Vebaere, Y. Piffard, M. Toumoux, Solid State Ionics 81 (1995) 167.
- [5] J.M. Tarascon, E. Wang, F.K. Sholooki, W.R. Mckinnon, S. Colson, J. Electrochem. Soc. 138 (1991) 2859.
- [6] Y. Xia, Y. Zhou, M. Yoshio, J. Electrochem. Soc. 144 (1997) 2593.
- [7] D.H. Jang, Y.J. Shin, S.M. Oh, J. Electrochem. Soc. 143 (1996) 2204.
- [8] D.H. Jang, S.M. Oh, J. Electrochem. Soc. 144 (1997) 3342.
- [9] J.M. Tarascon, W.R. Mckinnon, F. Coowar, T.N. Bowmer, G. Amatucci, D. Guyomard, J. Electrochem. Soc. 141 (1994) 1421.
- [10] D. Guyomard, J.M. Tarascon, Solid State Ionics 69 (1994) 222.
- [11] Y. Xia, M. Yoshio, J. Power Sources 57 (1995) 125.

- [12] Y. Xia, M. Yoshio, *J. Electrochem. Soc.* 143 (1996) 825.
- [13] Y. Gao, J.R. Dahn, *Solid State Ionics* 84 (1996) 33.
- [14] Y. Gao, J.R. Dahn, *J. Electrochem. Soc.* 143 (1996) 100.
- [15] H.H. Huang, C.A. Vincent, P.G. Bruce, *J. Electrochem. Soc.* 146 (1999) 481.
- [16] Y. Ein-Eli, J.T. Vaughty, M.M. Thackeray, S. Mukerjee, X.Q. Yang, J. McBreen, *J. Electrochem. Soc.* 146 (1999) 908.
- [17] J.H. Lee, J.K. Hong, D.H. Jang, Y.K. Sun, S.M. Oh, *J. Power Sources* 89 (2000) 7.
- [18] N. Hayashi, H. Ikuda, M. Wakihara, *J. Electrochem. Soc.* 146 (1999) 1351.
- [19] Y. Ein-Eli, W.F. Howard, *J. Electrochem. Soc.* 144 (1997) L205.
- [20] B.J. Hwang, R. Santhanam, D.G. Liu, *J. Power Sources*, 2001, in press.
- [21] B.J. Hwang, R. Santhanam, D.G. Liu, *J. Power Sources*, 2001, in press.